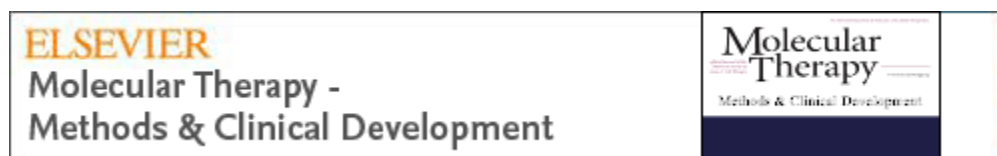


As a library, NLM provides access to scientific literature. Inclusion in an NLM database does not imply endorsement of, or agreement with, the contents by NLM or the National Institutes of Health.

Learn more: [PMC Disclaimer](#) | [PMC Copyright Notice](#)



Mol Ther Methods Clin Dev. 2025 Jan 28;33(1):101424. doi: [10.1016/j.omtm.2025.101424](https://doi.org/10.1016/j.omtm.2025.101424)

Preclinical development of TAK-754, a high-performance AAV8-based vector expressing coagulation factor VIII

[Johannes Lengler](#)^{1,4}, [Markus Weiller](#)^{1,4}, [Franziska Horling](#)^{1,4}, [Josef Mayrhofer](#)¹, [Maria Schuster](#)¹, [Falko G Falkner](#)¹, [Irene Gil-Farina](#)², [Matthias Klugmann](#)¹, [Friedrich Scheiflinger](#)^{1,3,*}, [Werner Hoellriegel](#)¹, [Hanspeter Rottensteiner](#)¹

[Author information](#) [Article notes](#) [Copyright and License information](#)

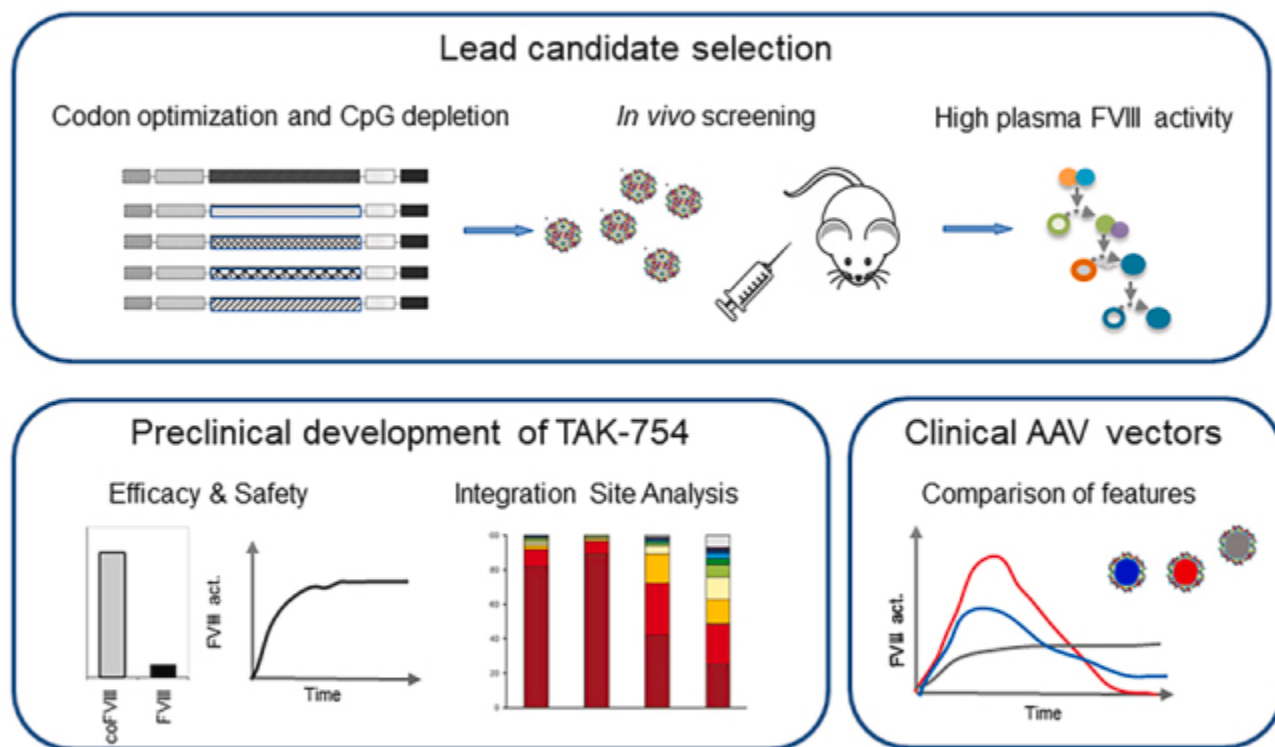
PMCID: PMC11929063 PMID: [40123744](#)

Abstract

This report concerns the preclinical development of TAK-754, an AAV8-based human factor VIII (FVIII) vector designed to deliver a codon-optimized and CpG-depleted B domain-deleted *F8* transgene under the control of a liver-specific promoter for gene therapy in patients with hemophilia A. A dose-dependent increase in plasma FVIII activity was detected in FVIII knockout mice at a dose of 1.0×10^{12} TAK-754 capsid particles (CP)/kg or higher. This increase was shown to be in accordance with a dose-dependent decrease in blood loss in a hemostatic efficacy assay. TAK-754 (3.1×10^{12} CP/kg) mediated long-term and stable FVIII expression in immunologically tolerant transgenic human FVIII mice. Toxicology and biodistribution assessments with a single administration of TAK-754 ranging between 1.9×10^{12} and 5.0×10^{13} CP/kg were conducted in male C57BL/6J mice. The highest TAK-754 dose occurred without TAK-754-related adverse clinical signs. Biodistribution profiling showed predominant detection in the liver with a low occurrence of vector DNA in other tissues. Integration site analysis revealed minimal vector integration, with no observations of clonal outgrowth or preferred integrations in genes previously implicated in hepatocellular carcinoma formation within the observation period. These preclinical studies demonstrate a good safety and efficacy profile for TAK-754.

Keywords: hemophilia A, gene therapy, adeno-associated virus, AAV, FVIII, biodistribution, safety, vector integration, vector immunogenicity

Graphical abstract



[Open in a new tab](#)

Lengler and colleagues report promising preclinical efficacy and safety of the TAK-754 hemophilia A gene therapy vector. Its vector design is compared with other clinical-stage AAV vectors to identify features that contribute to durable FVIII expression, thereby enabling the success of hemophilia A gene therapy.

Introduction

Hemophilia A is a monogenic X chromosome-linked inherited bleeding disorder caused by mutations in the *F8* gene encoding blood clotting factor VIII (FVIII), leading to the loss of functional FVIII protein.^{[1,2,3](#)} This lifelong disorder requires treatment with replacement factor concentrates to maintain FVIII levels to control and prevent bleeding episodes.^{[1,4](#)} Patients with severe disease can experience recurrent joint and muscle bleeding and may receive regular FVIII infusions to prevent the debilitating effects of arthropathy and to reduce their risk of life-threatening bleeds.^{[4,5](#)} Another more recent treatment option is the bispecific antibody emicizumab, which mimics FVIII function by binding FIXa and FX to promote hemostasis.^{[6](#)}

Monogenic diseases are promising indications for potentially curative gene therapeutic approaches,^{[7](#)} and in particular, hemophilia A has become a showcase indication for exploring and refining *in vivo* gene therapy principles.^{[8](#)} This is due to the fact that the expression of FVIII from the introduced functional copy of the *F8* transgene into a patient's liver cells can be readily measured in plasma, and relatively low levels of FVIII are already sufficient to alleviate a severe disease phenotype. For adeno-associated virus (AAV) vectors, this needs to be accomplished by a truncated, B domain-deleted (BDD) variant of FVIII (BDD-FVIII) because of the restricted packaging capacity of AAV, which is 5 kb at the most, excluding the flanking inverted terminal repeat (ITR) regions. Nonetheless, ample preclinical experience has demonstrated the feasibility of this approach, which also leads to improvements in vector design.^{[9,10,11,12](#)}

Several investigational hemophilia A gene therapy products built on this concept are being tested clinically,^{[13](#)} and the most advanced program has already received marketing authorization (Valoctogene roxaparvovec), employing an AAV5 vector designed to express a human BDD-FVIII variant called FVIII-SQ.^{[14,15](#)} Three years of follow-up data demonstrated a sustained, clinically relevant benefit at doses of 4×10^{13} and 6×10^{13} vg (vector genomes)/kg, but also identified a decline in FVIII expression levels over time, suggesting that this therapy will not be lifelong.^{[15](#)} Other observations difficult to explain to date are the variability in expression between individuals at a given dose and between participants in phase 1/2 and phase 3.^{[15](#)} These observations have not been made in conceptually similar clinical hemophilia B gene therapy trials and appear to be associated with the nature of the transgene product, as synthesis of FVIII at high levels in hepatocytes is constrained and prone to trigger an unfolded protein response that could lead to cellular stress.^{[16](#)}

Past and present hemophilia trials further revealed that vector immunogenicity can negatively affect the durability of transgene expression,^{[17,18,19](#)} reflected in a drop or even loss of activity within the first couple of months after treatment that is often accompanied by a transient rise in liver enzymes. While ultimately a cytotoxic T cell response against the

capsid protein contributes to this phenomenon, other host immune responses elicited by the inherent immunogenic features of recombinant AAV (rAAV) vectors are likely to be involved.^{20,21} The presence of (an excess of) unmethylated cytosine-guanine dinucleotides (CpG) motifs in the vg is particularly important in that respect as CpG clusters, which are typically present only in microbials, act as pathogen-associated molecular patterns (PAMPs) in humans and can trigger an innate immune response. The removal of such CpG clusters from vg is therefore thought to be a key measure for dampening innate immune signals that eventually lead to deleterious adaptive immune responses.²²

Here, we describe preclinical development of the recombinant single-stranded (ss) gene therapy vector TAK-754 (formerly BAX 888 and SHP654; Baxalta US, Lexington, MA) designed for the treatment of patients with hemophilia A. The vector was built on the AAV8 capsid with a preferential liver tropism and engineered to deliver a human codon-optimized and CpG-depleted *BDD-F8* transgene under the control of a liver-specific transthyretin (TTR) promoter. This paper details the identification of the lead candidate vector ssAAV8.BDD-FVIII and reports on preclinical studies aimed at evaluating the efficacy and safety of the TAK-754 human gene therapy vector in mice.

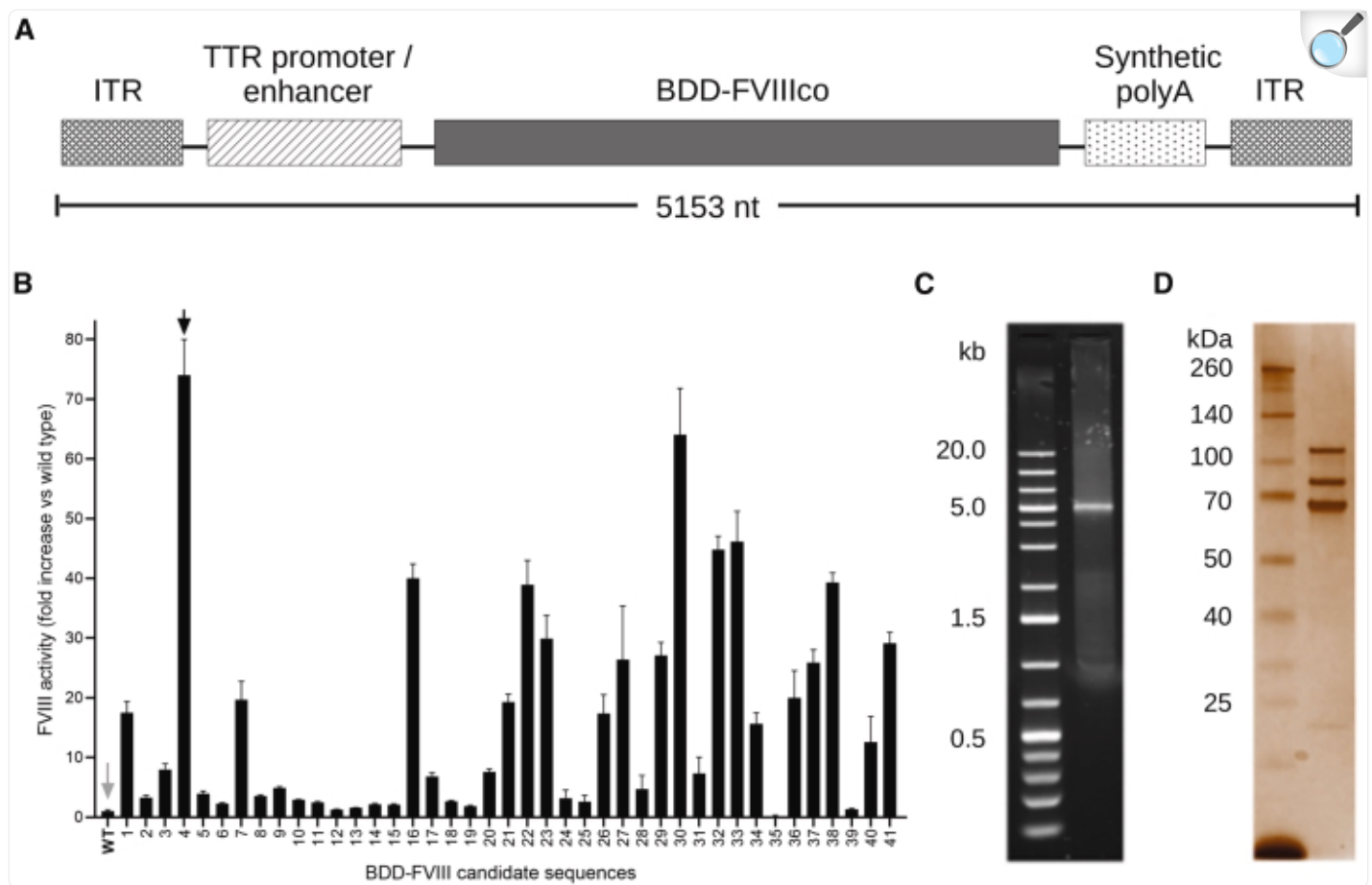
Results

Lead candidate screening of ssAAV8.BDD-FVIIIopt

Expression levels of endogenous wild-type (WT) FVIII levels are relatively low,²³ and the corresponding coding region exceeds the natural packaging limit for AAV. We addressed this by cloning codon-optimized *BDD-F8* open reading frames in an AAV expression cassette designed for high expression levels in human hepatocytes ([Figure 1A](#)). A total of 41 codon-optimized ssAAV8.BDD-FVIII vectors (sequences 01–41) were produced and screened for potency in FVIII knockout (KO) mice. FVIII KO mice closely reflect the severe hemophilia A phenotype in patients and therefore represent a suitable animal model. Expression was compared to animals receiving the ssAAV8.BDD-FVIIIwt control vector (sequence wt) harboring the WT *F8* nucleotide sequence. The best candidate of this *in vivo* biopotency screen was sequence (seq) 04, with 79.8% nucleotide sequence identity to the corresponding coding sequences in WT *F8* (GenBank: [M14113](#)) and 74-fold improved efficacy ([Figure 1B](#)). The guanine-cytosine (GC) content of seq04 was 56%, which is substantially higher than that of the WT sequence (44%) and matches the native AAV8 capsid protein coding sequence ([Figure S1](#); [Table S1](#)). Moreover, CpG motifs in seq04 were low in number and dispersed over the length of the transgene ([Figure S2](#)). This feature should help minimize the immunogenicity risk, as high densities of these DNA motifs can increase immunogenicity by stimulating the innate immune system via the Toll-like receptor (TLR) 9 in the liver.²⁴ Despite a vector size of approximately 5.2 kb, the recombinant genome appears as a single homogeneous band following DNA gel analysis ([Figure 1C](#)), confirming correct packaging of the slightly oversized genome of ssAAV8.BDD-FVIIIopt-seq04 (relative to an AAV WT genome of 4.7 kb). The same held true for the other AAV8.BDD-FVIII vectors (data not shown). Overall capsid integrity and purity of the ssAAV8.BDD-FVIIIopt-seq04 preparation was confirmed following SDS PAGE-based size separation and detection of VP1, VP2, and VP3 by silver staining ([Figure 1D](#)). Initial yields for the seq04 vector per liter cell culture were about 6-fold higher than for the

otherwise identical *F8* WT nucleotide sequence vector,^{[25](#)} indicating that vector production using the *F8* lead candidate sequence was actually more efficient, probably due to its GC content matching the GC content of the AAV8 virus ([Figure S1](#)).

Figure 1.



[Open in a new tab](#)

Candidate screening of AAV8.BDD-FVIIIopt

(A) Schematic drawing of the AAV cassette for expression of codon-optimized B domain-deleted *F8* cDNAs (*BDD-F8co*), including the liver-specific transthyretin (TTR) promoter/enhancer, a synthetic polyadenylation signal (polyA), and flanking AAV2 inverted terminal repeats (ITRs). (B) FVIII activity in plasma of FVIII KO mice ($n = 8$) at 2 weeks following i.v. delivery of 8.0×10^{12} vg/kg AAV8.BDD-FVIII vectors harboring different codon-optimized *BDD-F8* open reading frames. The nucleotide sequence with the best performance (seq04) is indicated by a black arrowhead and that of the WT control by a gray arrowhead. Data shown represent the mean \pm standard error of the mean (SEM). (C) Agarose gel analysis of the DNA payload of ssAAV8.BDD-FVIIIopt-seq4. Note the single band with the expected size of 5.2 kb. (D) SDS-PAGE of ssAAV8.BDD-FVIIIopt-seq4. The capsid proteins VP1, VP2, and VP3 appear as main proteins in the silver-stained gel.

These favorable features provided the rationale to select ssAAV8.BDD-FVIIIopt-seq04 as the lead candidate for the development of a hemophilia A gene therapy vector.

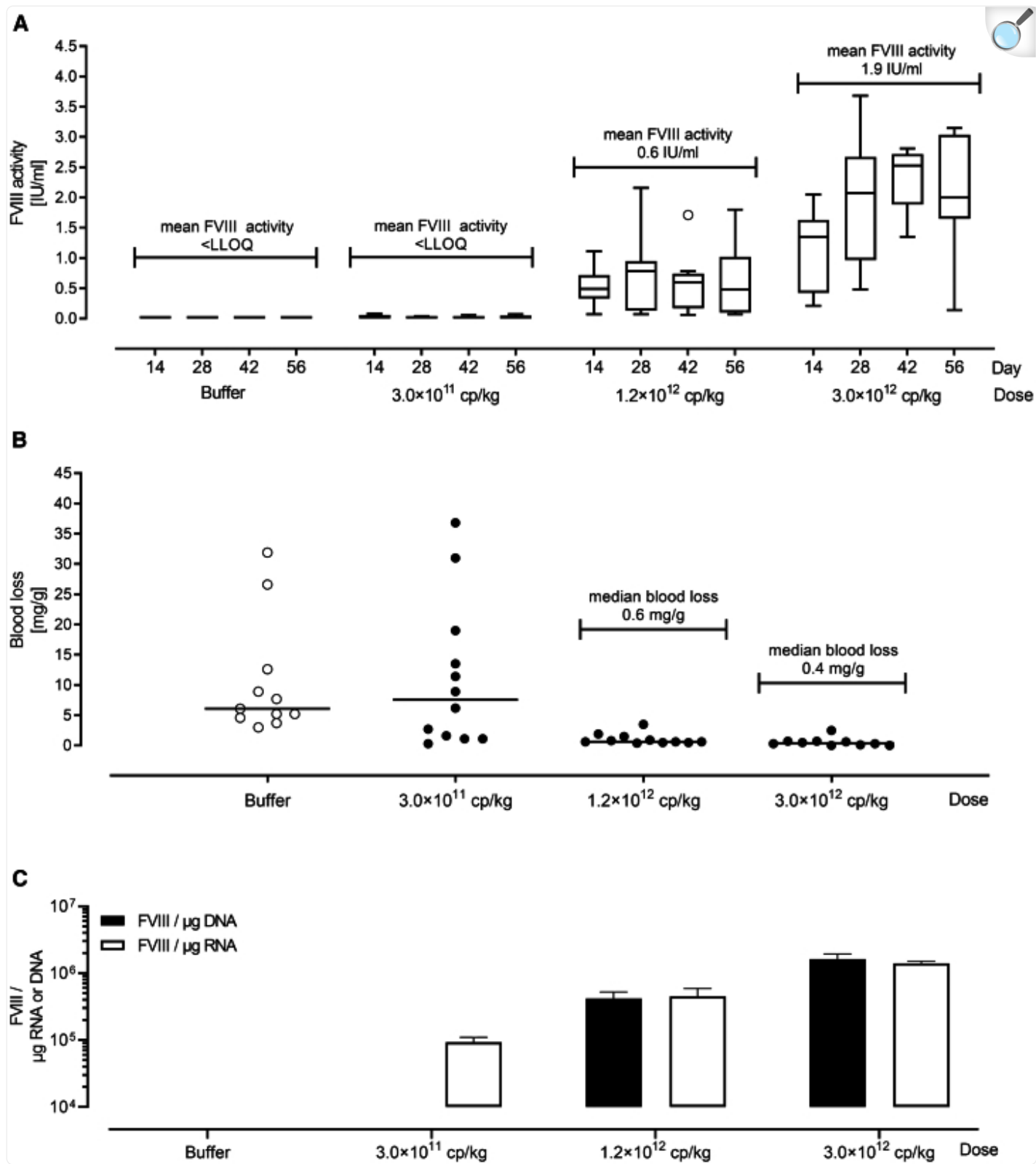
Biopotency and hemostatic efficacy of TAK-754

In anticipation of clinical trials of TAK-754 gene therapy in patients with hemophilia A, we optimized our vector titration approach, which was previously based on a qualified qPCR of vg with a coefficient of variation (CV) higher than 25% (data not shown). We therefore considered changing the genomic titering regime toward assaying AAV capsid particle (CP) numbers by ELISA, as the latter assay reproducibly showed a CV of <10%. The robust performance of the CP enzyme-linked immunosorbent assay (ELISA), together with a consistent full to empty capsid ratio of the vector batches produced,²⁶ provided the rationale to assign the vector strength for subsequent preclinical development of TAK-754, as well as for clinical dosing in a phase 1/2 study.

The FVIII activity dose response and hemostatic efficacy of TAK-754 was examined in FVIII KO mice following vector delivery at doses of 3.0×10^{11} , 1.2×10^{12} , or 3.0×10^{12} CP/kg. A preliminary safety assessment was included as a secondary endpoint. Animals that tested positive for anti-FVIII antibodies were excluded from statistical analysis of biopotency and efficacy. No treatment-related findings were observed microscopically in the heart, kidney, liver, or spleen, including micro- or macrovascular thrombosis or inflammatory infiltrate.

Animals that received 1.2×10^{12} or 3.0×10^{12} CP/kg showed a dose-dependent increase in mean plasma FVIII activity from 0.6 to 1.9 IU/mL over the investigation period ([Figure 2A](#)). FVIII activity was undetectable in animals treated with buffer or the lowest dose of 3.0×10^{11} CP/kg. Dose-dependent activity of TAK-754 was confirmed in the human hepatic HepG2 cell line ([Figure S3](#)).

Figure 2.



[Open in a new tab](#)

Potency and hemostatic efficacy of TAK-754

(A) *In vivo* biopotency determination. FVIII KO mice ($n = 12$) were injected with 3.0×10^{11} , 1.2×10^{12} , and 3.0×10^{12} CP/kg TAK-754 vector and analyzed for plasma FVIII activity at four time points, including 14, 28, 42, and 56 days. FVIII activity levels were below the lower limit of quantification (LLOQ) in controls and the low-dose group but showed a dose-dependent increase in the mid- and high-dose groups. Data are shown in box and whiskers plots, with the median indicated by a horizontal line. (B) Hemostatic efficacy testing. The same animals as under (A) were subjected to a tail tip bleeding assay on day 63. A dose-dependent reduction of blood loss was observed for the higher doses. Note that only animals testing negative for anti-FVIII antibodies on day 56 were tested. The median is indicated by a horizontal line. (C) Transduction efficiency. *F8* transgene copy numbers in gDNA (dark bars) and in cDNA (light bars) were quantified in TAK-754-treated animals and controls ($n = 2$) on day 63, confirming dose-dependent liver transduction. Data are presented as the mean \pm standard deviation (SD).

A tail-tip bleeding assay was used to assess the bleeding phenotype. Animals treated with buffer and TAK-754 at the lowest dose showed similar median blood loss normalized for body weights of 6.1 and 7.5 mg/g, respectively, corresponding to the undetectable FVIII activity in these animals ([Figure 2B](#)). The higher doses (1.2×10^{12} or 3.0×10^{12} CP/kg) of TAK-754 significantly reduced median blood loss to 0.6 and 0.4 mg/g, respectively, in a dose-dependent manner ($p < 0.001$ compared to buffer). Statistical assessment of dose proportionality was precluded by the lack of FVIII activity at the low dose.

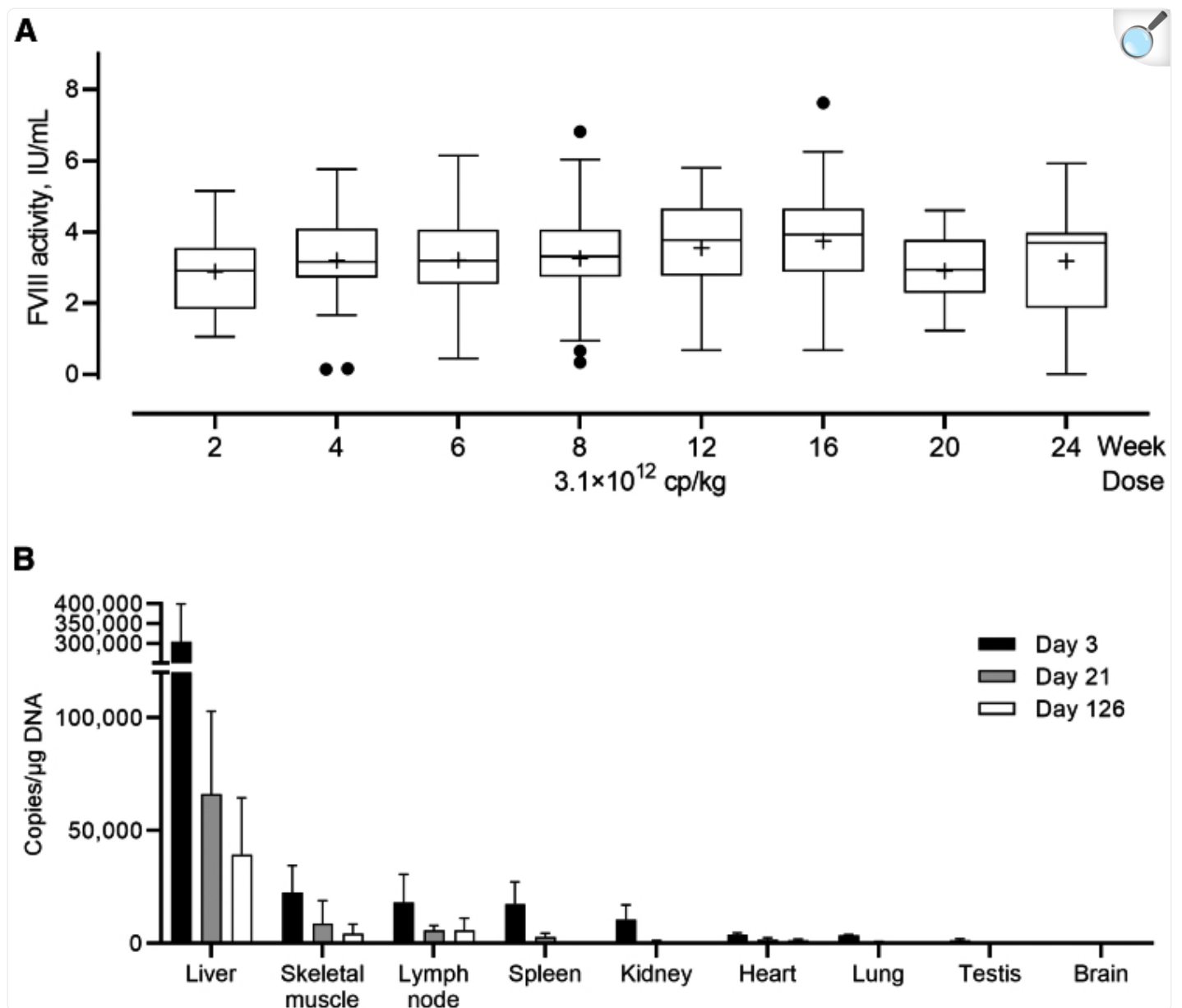
At the end of the experiment, livers of animals with activities around the mean FVIII activity were selected from each group for quantification of vg and *F8* RNA expression. The vg levels in the control group or the low-dose TAK-754 group were under the detection limit of the applied method. Mid- and high-dose animals showed robust and dose-dependent transduction as a function of vg in the liver ([Figure 2C](#)). *F8* RNA levels were consistent with *F8* DNA levels, except for two low-dose animals showing a measurable *F8* transcript signal (i.e., within the limit of detection). The 2.5-fold dose increase from 1.2×10^{12} to 3.0×10^{12} CP/kg resulted in a 3.9-fold increase in *F8* gDNA levels and a 3.1-fold increase in *F8* RNA levels ([Figure 2C](#)), which broadly mirrored the 3.2-fold increase in FVIII activity levels ([Figure 2A](#)).

TAK-754-mediated long-term expression of FVIII

The development of an antibody response directed against the human FVIII xenoprotein capable of neutralizing FVIII activity is a well-known phenomenon in mice.²⁷ To enable a long-term expression study following the delivery of TAK-754, we employed a transgenic mouse model (huFVIII tg mice) that lacks detectable FVIII protein but usually

shows immunological tolerance toward the human coagulation factor.²⁸ huFVIII tg mice were injected with a TAK-754 dose of 3.1×10^{12} CP/kg and were monitored for FVIII activity and anti-drug antibodies from 2 to 24 weeks. The mean FVIII plasma activity ranged between 2.9 and 3.8 IU/mL throughout the observation period ([Figure 3A](#)). Three of 30 animals tested positive for anti-BDD-FVIII immunoglobulin-binding antibodies. In one of these three animals, the antibody response appeared to be transient, as it tested negative in week 24. One of the two persistent binding antibodies-positive animals also tested positive for FVIII inhibitory antibodies (data not shown). No treatment-related clinical symptoms or deaths were recorded.

Figure 3.



[Open in a new tab](#)

Sustained FVIII expression following a single injection of TAK-754

(A) Long-term FVIII expression in a transgenic human FVIII mouse model. Following delivery of 3.1×10^{12} CP/kg of TAK-754 to huFVIII tg mice ($n = 30$), activity levels were stable between 2 and 24 weeks. Data are presented in box and whiskers plots, with the median indicated by a horizontal line and the mean represented by a cross. (B) Vector biodistribution. Wild-type C57Bl/6J mice were treated with a TAK-754 dose of 9.5×10^{12} CP/kg, and vector biodistribution was determined at three time points, including 3 days, 3 weeks,

and 18 weeks ($n = 20$). Data are given in mean \pm SEM; values $<$ LLOQ were included as zero.

Nonclinical safety evaluation and biodistribution study in hemostatically normal mice

The toxicity of gene therapy candidate TAK-754 was examined in cohorts of male C57BL/6J mice receiving a single dose of TAK-754 at 2.0×10^{12} , 3.8×10^{12} , and 9.5×10^{12} CP/kg, and also at higher dose levels up to 5.0×10^{13} CP/kg (1.0×10^{13} , 3.0×10^{13} , and 5.0×10^{13} CP/kg). The dose levels were selected based on the TAK-754 activity data shown in [Figure 2A](#). The design of the toxicity study entailed subjecting cohorts of animals to a panel of analyses that included complete necropsies, pathological evaluation, biodistribution of vg, FVIII activity, FVIII antigen, binding anti-BDD-FVIII antibodies, neutralizing anti-BDD-FVIII antibodies, and binding anti-AAV8 antibodies at day 3, week 3, and week 18.

During the study, there were no deaths and no adverse effects attributed to TAK-754 during the in-life phase, pathology, post-dosing observations, or any adverse TAK-754-related changes in clinical chemistry parameters, hematology, and coagulation parameters or urinalysis.

The distribution of TAK-754 DNA was highest in the liver at all dose levels tested. TAK-754 distribution in liver and other tissues was dose related and was generally highest at the earliest time point, decreasing by day 21 ([Figure 3B](#)). However, TAK-754 DNA levels were still highest in liver tissues at this time point. Further decrease by day 126 is already diminished in the liver and skeletal muscle and not observed in lymph node and heart any longer. TAK-754 DNA levels in brain and testes samples harvested from TAK-754-treated animals were evaluated as negative or below the lower limit of assay quantification by week 18 in all animals. Representative data are shown from the 9.5×10^{12} CP/kg dose group ([Figure 3B](#)).

Animals treated with TAK-754 had measurable amounts of human FVIII antigen in plasma from week 3, with levels in some mice already present from day 3. The observed decrease in FVIII antigen concentrations in individual animals was most likely a result of the formation of circulating anti-human BDD-FVIII binding antibodies, which can compete with the species-specific assay, resulting in nondetectable FVIII antigen. Such binding antibodies indeed formed over time and increased with dose, which is in line with a pharmacokinetic analysis where FVIII immunogenicity increased with initial high-level AAV-FVIII protein expression.^{[29](#)}

TAK-754-treated animals also showed higher FVIII activity levels compared with the pre-treatment period, indicating that BDD-FVIII was expressed in these mice. However, some animals had even lower-than-normal FVIII levels most likely caused by the generation of neutralizing anti-human-BDD-FVIII antibodies that inhibited both human BDD-FVIII

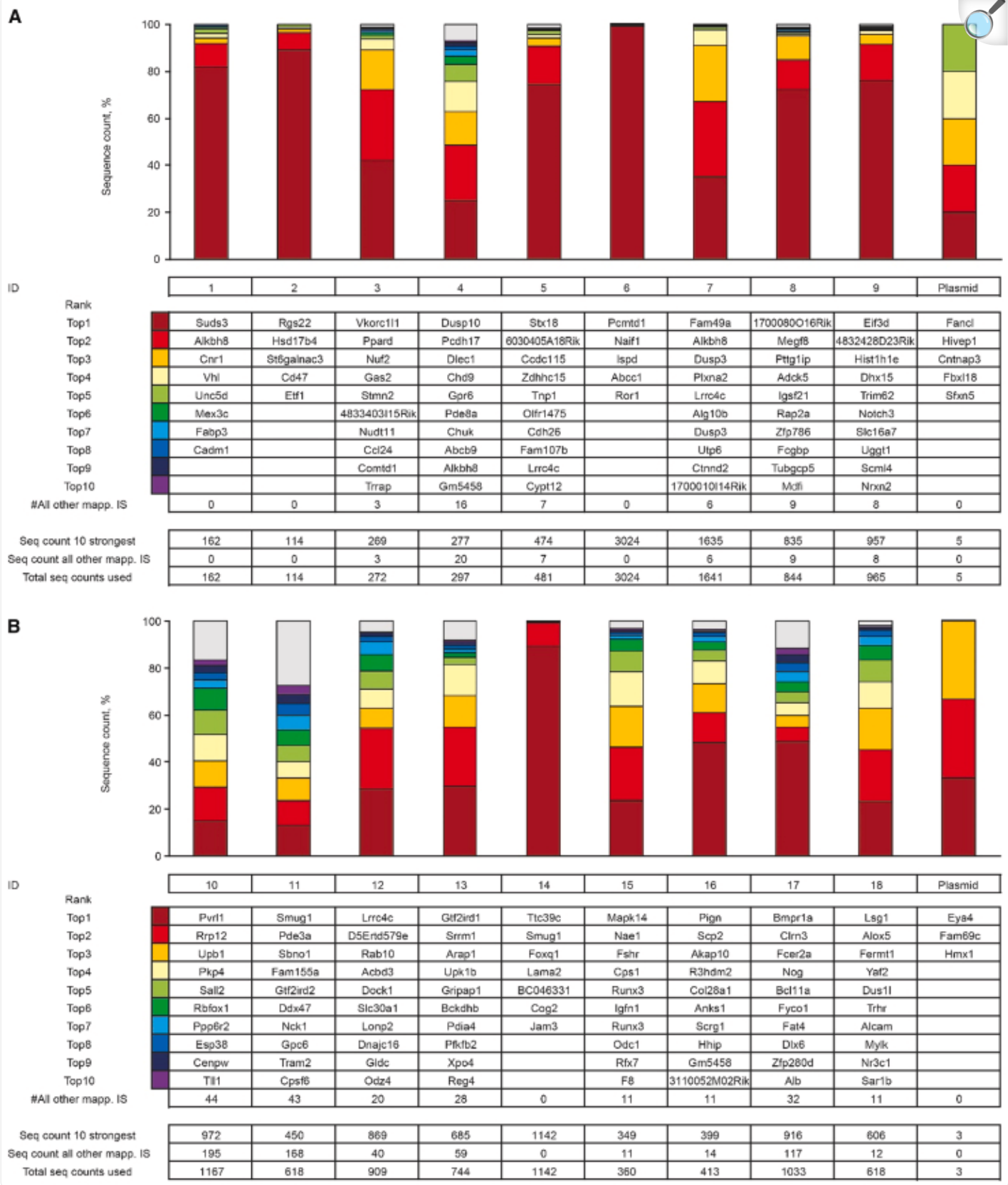
activity and endogenous mouse FVIII activity by virtue of the antibodies' partial cross-reactivity against mouse FVIII. Neutralizing antibodies against BDD-FVIII became measurable by week 18 in all dose groups. As expected, all treated animals tested strongly positive for anti-AAV8 binding antibodies from week 3.

In summary, toxicology experiments in mice receiving single intravenous (i.v.) TAK-754 injections at doses up to 5.0×10^{13} CP/kg found no evidence of TAK-754-related adverse effects during the in-life phase and no toxicologically relevant observations. The no-observed-adverse-effect level was 5.0×10^{13} cp/kg, the highest dose tested.

Integration site analysis

While host cell maintenance of rAAV vectors is largely accomplished through episomal DNA, residual chromosomal integration does occur. We therefore performed an integration site (IS) analysis of the TAK-754 vector in FVIII KO mice. Mice were treated with either 2.0×10^{12} or 1.0×10^{13} CP/kg TAK-754 and observed for 1 or 4 months ([Figure 4](#)). Liver transduction levels, determined by *F8* qPCR, were dose dependent and comparable at both time points ([Figure S4](#)).

Figure 4.



Vector integration site analysis

Cumulative retrieval frequencies of top 10 cell clones in the livers of mice following injection of TAK-754 at (A) 2.0×10^{12} or (B) 1.0×10^{13} CP/kg. Samples with ID 1–4 and 10–13 were analyzed 1 month after treatment, those with ID 5–9 and 14–18 four months after treatment.

Illumina sequencing of nonrestrictive (nr)linear amplification-mediated (LAM)-PCR products showed comparable numbers of average sequencing reads for both time points after vector administration ([Table S2](#)). A total of 227 unique exactly mappable ISs were detected in animals in both groups at 1 month after gene therapy treatment (5–54 unique ISs/mouse). Four months after treatment, 187 unique exactly mappable ISs were retrieved from both groups (5–42 unique ISs/mice), confirming an integration frequency of $\leq 0.01\%$ ([Table S2](#)).

The detection of identical top 10 ranking ISs in repetitive (nr)LAM-PCR amplicons was very low: one IS 1 month after treatment and 3 ISs detected in 2/6 (nr)LAM-PCRs after 4 months ([Figure 4](#)). This indicates that the unequal IS frequency profiles are due to the low number of events retrieved and that there are no signs for clonal skewing or clonal dominance in the treated animals. Only low-order (≤ 4) common ISs could be identified at both time points, which is in line with the low number of ISs detected after administration of TAK-754, correlating with an untargeted integration profile. None of the ISs were found in or next to genes previously implicated in hepatocellular carcinoma (HCC) formation.³⁰

In summary, the integration profile of TAK-754 in FVIII KO mouse liver showed a low but measurable level of integration, with no signs of potential side effects, and, at least within the 4-month observation period, no evidence for clonal outgrowth or preferred integrations in oncogenes (i.e., HCC) was noted.

Discussion

Here, we describe preclinical development of TAK-754, an efficient human AAV vector for gene therapy in patients with hemophilia A, designed to express a human BDD-FVIII protein with an identical amino acid sequence to that of recombinant FVIII moroctocog alfa.³¹ While the vector was designed and developed at a time before first clinical readouts from hemophilia A gene therapy trials became available, it does bear a couple of features that should allow efficient expression of the human *F8* transgene in humans.

TAK-754 vector design

Choice of the AAV8 capsid was based on its preferential tropism for the liver as it demonstrates excellent transduction efficiency of hepatocytes in preclinical models³² and a number of liver-directed clinical gene therapy trials such as those for the treatment of hemophilia A and B or glycogen storage disease type 1A build on this capsid serotype.³³ Numerous comparative studies over the last couple of years consolidated our comprehension of a species-dependent performance of vector capsids.³⁴ It is now clear that AAV8 is particularly efficient in rodents; in nonhuman primates (NHPs) and humans, the capsid also preferentially targets hepatocytes but with an approximately 20-fold lower efficiency.³⁵ This correlation factor needs to be considered when it comes to the deduction of a clinical starting dose from the nonclinical data package. Accordingly, a starting dose of 2.0×10^{12} CP/kg TAK-754 vector was selected for the first cohort, taking into account that a dose of 3.0×10^{12} CP/kg in FVIII KO mice resulted in a mean plasma FVIII activity of 1.9 IU/mL, translating into a projected clinical FVIII activity of ~6% of normal.

It is worth noting that the packaging capacity of recombinant AAV8 vectors can be pushed beyond the size of the WT genome of 4.7 kb.³⁶ Consistently, we found that TAK-754's vg was the correct size and intact, as judged by the absence of degradation bands. Packaging of similarly oversized BDD-FVIII expression cassettes using AAV5³⁷ and AAVrh8³⁸ led to aberrant, truncated genomes that first had to be re-assembled in transduced cells through recombination before functional FVIII could have been produced.

The use of the strong yet compact mouse TTR promoter/enhancer combination enabled robust liver-specific gene expression. This promoter was selected from a variety of liver-specific promoters during preclinical development of the hemophilia B vector BAX335³⁹ and came off well in a head-to-head comparison with other commonly used liver-specific promoters.⁴⁰ The risk of relying on nonconserved murine transcription factor binding sites for a human gene therapy was mitigated by our demonstration of robust BDD-FVIII expression in the human liver HepG2 cell line upon transduction with TAK-754. Activity of the mouse TTR promoter/enhancer was also confirmed in the clinical trials for BAX335¹⁸ and SPK-8011,⁴¹ although in the latter case, a point-mutated promoter variant was used that has converted a weak hepatocyte nuclear factor 3 (HNF3) binding site into a moderately stronger one.

Codon optimization of the *BDD-F8* transgene initially relied on available codon-optimization algorithms. This approach resulted in sequences with improved expression but also greater GC content, in line with the understanding that this leads to higher mRNA levels and greater protein translation than gene sequences having greater AT content.⁴² However, this inadvertently introduced CpG clusters into the vector sequence, which function as PAMPs. These sequences can stimulate innate immune responses through signaling via TLRs, leading to an exaggerated adaptive immune response.^{22,43,44} TAK-754 candidate screening thus included a further filtering step that removed codon-optimized *F8* sequences harboring potentially detrimental predicted CpG clusters.⁴⁵ The lead candidate *F8* nucleotide sequence (seq04) gave rise to a 74-fold increased expression in FVIII-KO mice compared to the corresponding WT sequence yet contains only 17 dispersed CpG motifs (Figures S2A and S2B). A further depletion of CpG motifs within the entire expression cassette, which may likewise be important for durable transgene expression,¹³ has not been carried out (Figure S2B).

Preclinical evaluation of TAK-754

Overall, the vector showed a good efficacy and safety profile. Dose-dependent increases in mean plasma FVIII activity were obtained after single i.v. injections of TAK-754 in FVIII KO mice. The observed variability of FVIII expression ([Figure 2A](#)) appears to be a transgene-specific phenomenon. While FIX expression is associated with a low inter-species variability,^{[46](#)} that of BDD-FVIII is consistently higher and observed in mice and humans. Reports investigating the underlying mechanisms of inter-individual variability of AAV5-hFVIII-SQ (Valoctocogene roxaparvovec) expression concluded that multiple host-mediated factors could contribute.^{[47,48](#)} Future endeavors to identify predictive biomarkers of response might lead to the development of approaches with optimized outcomes of AAV-based *F8* gene therapies.

A TAK-754-mediated dose response of FVIII activity was confirmed in a HepG2 cellular biopotency assay. Such an *in vitro* assay could allow replacement of the cumbersome *in vivo* lot release testing procedure, in line with the expectations and requirements of the authorities, which support the reduction and circumvention of animal experiments in the release of clinical batches, if applicable.^{[49](#)}

Dose-dependent efficacy was observed in the tail tip bleeding assay in FVIII KO mice, and long-term expression could be demonstrated in a separate animal study using human FVIII transgenic mice, in which a single dose of 4×10^{12} CP/kg resulted in FVIII expression from week 2 until the end of the experiment (6 months), with no trend for a decline in FVIII activity. This mouse model, which was developed to mitigate the issue of anti-human FVIII antibody formation,^{[28](#)} served its purpose to monitor TAK-754-dependent long-term expression of human BDD-FVIII. While this model also allows comparative prediction of human immune responses elicited by human FVIII variants via repeated dosing of the respective recombinant proteins according to identical protein mass, this study setup could not be mirrored with a gene therapy vector. Due to the further absence of a gold standard vector regarding FVIII immunogenicity, we did not aim for conducting a comparative FVIII immunogenicity study with the TAK-754 vector. It is important to note that the model falls short in predicting the FVIII expression decline based on AAV vector immunogenicity, which is a phenomenon known to be largely absent from typical preclinical animal models.

No toxicologically relevant effects related to TAK-754 were observed. Single bolus injections of TAK-754 administered to mice at doses of up to 5×10^{13} CP/kg occurred without deaths, adverse clinical signs, or post-dosing observations related to TAK-754. A limitation of the mouse safety study was its duration of 18 weeks, which precluded the detection of a potential relationship between FVIII expression and liver cancer/hyperplasia, which can occur at time points later than 1 year.^{[50](#)}

The observed biodistribution of TAK-754 in treated FVIII KO mice confirmed the predominant detection of vector DNA in liver tissue, with minimal off-target gene expression in other tissues, consistent with the hepatic tropism of AAV8. Despite the known technical limitations of (nr)LAM-PCR, IS analyses further showed that vector integration was minimal (<0.01%). Within the 4-month observation period, there were also no observations of clonal outgrowth or

preferred integrations in or near genes previously implicated in HCC formation. While these data suggest that in humans TAK-754 will be maintained episomally and pose a low genotoxicity risk to patients, caution is needed since HCC-relevant loci are not well conserved between mice and humans,³⁰ and the duration of the study was too short to observe any HCC concerns.

Perspective

The preclinical development program showed a good efficacy and safety profile for TAK-754 and formed the basis for defining the starting dose of 2.0×10^{12} CP/kg, factoring in the above-mentioned mouse-to-human correlation factor for AAV8. Despite these promising data, based on the gathered clinical experience with liver-directed AAV gene therapies over the last couple of years, it has turned out that vector immunogenicity in humans appears more critical than in rodents or NHPs.⁵¹ A successful translation of preclinical gene therapy programs into the clinic critically depends on the type and strength of the immune responses elicited against the very gene therapy vector in humans. In the case of TAK-754, while the safety profile was consistent with an AAV8-based gene therapy and all four enrolled patients in the clinical trial (this study was registered at ClinicalTrials.gov: [NCT03370172](https://clinicaltrials.gov/ct2/show/study/NCT03370172)) showed dose-dependent peak FVIII activity 4 to 9 weeks after infusion (cohort 1: 2.0×10^{12} CP/kg [$n = 2$]: 3.8% and 11%, respectively; cohort 2: 6.0×10^{12} CP/kg [$n = 2$]: 54.7% and 69.4%, respectively), the initial vector-derived FVIII expression steadily declined despite the use of corticosteroids.⁵² The comprehensive analysis of immune components in the peripheral blood of the patients did not reveal the presence of inhibitory anti-FVIII antibodies or any obvious signs of an exaggerated immune response.⁵³

It is worth mentioning in this context that NHPs as a nonrodent species were excluded from preclinical safety testing mainly because of technical challenges such as the naturally high AAV8 infection rate in monkey populations.^{54,55} Since an AAV vector-induced immune response leading to an abrupt or gradual loss in FVIII expression has not been observed in NHPs,⁵⁶ such a study would also likely have failed to reveal an issue with the TAK-754 vector already in preclinical stage.

A comparison with Valoctocogene roxaparvovec and other clinical-stage hemophilia AAV vectors ([Table 1](#)) suggests that rather subtle yet not fully understood differences in the vector design determine the success or failure of a therapy.¹³ Several AAV-based hemophilia A gene therapy clinical trials registered on [ClinicalTrials.gov](https://clinicaltrials.gov) also counted on AAV8, whereas other programs use different capsids, including AAV5, AAV6, LK03, and AAVhu37, with potential differences in their tropism or transduction efficiency. Ranking these capsids in terms of performance in humans is, however, difficult since all these vectors differ also in expression cassette design and manufacturing process employed. Clinical head-to-head comparisons of vectors differing only in the capsid serotype are lacking and would be difficult to conduct for various reasons such as cross-reactivity of anti-AAV antibodies against a broad range of serotypes.

Table 1.

Characteristics of hemophilia A clinical stage AAV gene therapy vectors

| Product | Sponsor | AAV serotype | Transgene product | Expression cassette | No. of CpGs | GC content, % | Production platform |
|---------------------------------------|--------------------|--------------|----------------------------------|---|----------------|--------------------|---------------------|
| TAK-754 | Takeda | AAV8 | <i>BDD-hFVIII-SQ^a</i> | liver-specific TTR enhancer/ promoter codon- optimized <i>BDD-hF8-SQ</i> synthetic poly(A) | 17 | 55.94 | HEK293 |
| Valoctocogene roxaparvovec | Biomarin | AAV5 | <i>BDD-hFVIII-SQ</i> | liver-specific ApoE/A1AT promoter codon- optimized <i>BDD-hF8-SQ</i> synthetic poly(A) | 3 ^b | 57.70 ^b | Sf9/ baculovirus |
| Dirloctocogene samoparvovec (SPK8011) | Spark Therapeutics | LK03 | <i>BDD-hFVIII-SQ</i> | liver-specific TTRm enhancer/ promoter with mutated HNF3 binding site synthetic intron codon- optimized | 0 ^c | 52.47 ^c | HEK293 |

| Product | Sponsor | AAV serotype | Transgene product | Expression cassette | No. of CpGs | GC content, % | Production platform |
|--|------------------|--------------|-----------------------------------|--|------------------|--------------------|---------------------|
| | | | | <i>BDD-hF8-SQ</i> | | | |
| | | | | synthetic poly(A) | | | |
| Giroctocogene fitelparvovec (PF-07055480/SB-525) | Pfizer/Sangamo | AAV6 | <i>BDD-hFVIII-SQ</i> | liver-specific synthetic promoter codon-optimized <i>BDD-hF8-SQ</i> | 40 _d | 56.56 _e | Sf9/baculovirus |
| | | | | synthetic poly(A) | | | |
| Peboctocogene camaparvovec (BAY 2599023/DTX-201) | Bayer/Ultragenyx | AAVhu37 | <i>BDD-hFVIII-SQ</i> | liver-specific E03-TTR enhancer/promoter codon-optimized <i>BDD-hF8-SQ</i> | 185 _f | 56.05 _f | HeLa |
| | | | | synthetic poly(A) | | | |
| GO-8 | UCL/St. Jude | AAV8 | <i>BDD-hFVIII-V3</i> _g | liver-specific HLP promoter codon-optimized <i>BDD-hF8-V3</i> | 3 _b | 58.34 _b | HEK293T |
| | | | | synthetic poly(A) | | | |
| ASC618 | ASC Therapeutics | AAV8 | <i>ET3</i> _e | liver-specific synthetic HCB promoter | 0 _h | 50.8 _h | HEK293 |

| Product | Sponsor | AAV serotype | Transgene product | Expression cassette | No. of CpGs | GC content, % | Production platform |
|---------|---------|--------------|-------------------|----------------------------|-------------|---------------|---------------------|
| | | | | codon optimized <i>ET3</i> | | | |
| | | | | synthetic poly(A) | | | |

[Open in a new tab](#)

ApoE/A1AT, apolipoprotein E/alpha-1-antitrypsin; HCB, hepatic combinatorial bundle; HLP, hybrid liver-specific promoter; HNF3, hepatocyte nuclear factor 3; TTRm, mutated transthyretin.

^aReference [31](#), BDD-hFVIII, with 14-amino acid SQ linker (moroctocog alfa).

^bPatent US9447168B2.

^cReference [41](#).

^dPatent US20240066146A1.

^ePorcine-human BDD-FVIII hybrid protein.

^fPatent US10888628B2.

^gReference [9](#), BDD-hFVIII, with 17-amino acid peptide insertion comprising 6 N-linked glycosylation motifs.

^hReference [11](#).

With regard to the expression cassettes, all vector products rely on liver-specific promoter/enhancer combinations, with SPK8011 even using the same mouse TTR promoter, albeit with a point mutation in the HNF3 binding site reported to moderately increase transcription.[41](#) The SPK8011 cassette is unique in harboring a short synthetic intron, which is likely to further improve transgene expression. All but two (GO-8 and ASC618) transgenes were designed to express recombinant FVIII moroctocog alfa,[31](#) although different algorithms for codon optimization were likely used, which may substantially affect expression efficiency. No relevant differences in expression levels are expected from the poly(A) elements, all of which are short and synthetic in nature.

From the publicly available data, it appears that not all codon-optimized BDD-*F8* transgene cDNAs have been depleted for CpG motifs ([Table 1](#)). Whether the remaining 17 CpG motifs in TAK-754 caused a more pronounced vector-mediated immune response compared to that of SPK8011 (0 CpG) or Valoctocogene roxaparvovec (3 CpGs) is difficult to evaluate, but it seems unlikely as they are dispersed and do not form a CpG cluster.[45](#) Both the design of the expression cassette as well as the clinical data available so far suggest that SPK8011 is the most efficient vector, enabling expression of BDD-FVIII at a dose that falls within the tolerated capsid immune response window.

At the same time, however, it transpired over the last several years that FVIII expression should be kept at a moderate level so as to avoid an unfolded protein response in the transduced cells, leading to a decline in FVIII activity.^{[13](#),[57](#)} Efforts to optimize AAV-based *F8* gene therapy should therefore focus on bioengineered FVIII constructs with a lower propensity to misfold in the endoplasmic reticulum,^{[58](#),[59](#)} accompanied by target tissue-specific analysis and development of improved preclinical immunogenicity models, which in turn will increase the field's understanding of the key features that make up an effective gene therapy product for hemophilia A.

Materials and methods

AAV expression cassettes and vector production

For candidate screening, codon-optimized cDNAs encoding the amino acid sequence identical to recombinant FVIII moroctocog alfa-type BDD-FVIII^{[31](#)} were used to generate AAV expression cassettes that were composed of flanking AAV2-derived ITRs, a liver-specific TTR promoter/enhancer,^{[60](#)} the respective *BDD-F8* transgene, and a synthetic polyadenylation site.^{[61](#)} Recombinant ssAAV8 vectors were produced in suspension HEK293 cells using a triple plasmid transfection protocol as described.^{[62](#)} Titers of AAV vectors were determined by quantitative polymerase chain reaction (qPCR) or ELISA, reported in vg/mL or CP/mL, respectively.

vg titer determination

Vector genomes were quantified by qPCR targeting the AAV2 ITR sequence as described.^{[63](#)} Sample preparation prior to PCR included treatment of vector solutions with DNaseI, followed by a Proteinase K step to release the AAV genome from the capsid. A final restriction enzyme digest with SmaI was performed to resolve AAV ITR T-shape structures.

AAV titer determination by ELISA

The commercially available ELISA (Progen AAV8 titration ELISA kit) contains a monoclonal antibody (ADK8) specific for a conformational epitope on assembled AAV8 capsids. The AAV8 capsid concentration was determined photometrically using plate-immobilized biotinylated anti-AAV8 antibodies.

Vector DNA integrity assay

The integrity of the vg was analyzed by AAV agarose gel electrophoresis performed as described.^{[64](#)} Briefly, 1.5×10^{10} vg/lane were electrophoresed in agarose gels, which were then stained in 2× GelRed solution (Biotium) and imaged.

SDS-PAGE and silver staining

SDS-PAGE followed by silver staining was performed according to standard procedures. Each lane contained 1.0×10^{10} vg of the respective viral construct and was separated on a 4%–12% Bis-Tris gel (NuPAGE Novex, Thermo Fisher Scientific). Silver staining was performed with a SilverQuest kit (Novex, Thermo Fisher Scientific).

Animals

All animal experiments were approved by the relevant authorities on animal experiments and the Institutional Animal Care and Use Committee. The experiments were performed with male mice only. Three different strains were used: hemostatically normal C57BL/6J mice (Charles River Laboratories) for the Good Laboratory Practice toxicity study according to International Conference on Harmonization S6, FVIII KO mice (B6; 129S4-*F8tm2Kaz*; E17 KO)⁶⁵ for short-term biopotency and efficacy studies, where animals with an immune response against the human FVIII xenoprotein were excluded from further evaluation, and hFVIII transgenic mice²⁸ for the long-term expression study. In the latter strain, the murine *F8* gene is knocked out, but it also expresses human FVIII mRNA transcripts in multiple tissues from transgenic human *F8* cDNA while lacking detectable circulating FVIII protein.

Vector administration

TAK-754 was administered with 0.01% human serum albumin to mice aged 8–11 weeks via manual injection into the lateral caudal vein (tail). A dose volume of 10 mL/kg was used, and individual dose volumes were based on the individual body weight. An infusion rate of approximately 2 mL/min was used.

Blood sampling

Immediately prior to blood collection, animals were anesthetized with isoflurane. We collected 250-μL blood samples via puncture of the retro-orbital plexus. At the end of the in-life phase, an additional and terminal cardiac blood sample (0.8 mL) was collected from anesthetized animals. All blood samples were collected directly in citrate anticoagulants and processed by centrifugation within 15 min.

Detection of hF8 DNA or RNA in mouse organs

Genomic DNA (gDNA) or total RNA was extracted from mouse livers using the DNeasy Blood & Tissue Kit (Qiagen) or the RNeasy mini kit (Qiagen), respectively, following the manufacturer's protocol for animal tissues. gDNA was quantified using the Qubit dsDNA Broad-Range Kit (Thermo Fisher Scientific). Total RNA (1 μg) was treated with

DNase (TURBO DNA-free Kit, Thermo Fisher Scientific), and complementary DNA (cDNA) was synthesized using the SuperScript III First-Strand Synthesis SuperMix kit (Thermo Fisher Scientific). *F8*-transgene copy numbers in both gDNA and cDNA samples were determined by qPCR. The nucleotide sequences of the primers and probe used are the following: forward primer 5'-TCATGGACACCCTGCCT-3'; reverse primer 5'-GAGAAGTGGATGGAGTGAATGT-3'; probe 5'-6-FAM-ACCTGCTTTCTATGGGCTCCAATGAG-MGB-3'. PCR reactions were carried out on the QuantStudio 7 Flex PCR platform (Thermo Fisher Scientific). qPCR data analysis was performed using the specific device's software that automatically calculates the *F8* copies per reaction based on the linear regression parameters of the standard curve.

In vivo FVIII biopotency assay

FVIII activity in plasma was determined using a commercial FVIII chromogenic assay according to the manufacturer's instructions (COATEST SP4 FVIII; catalog no. 82409463, Chromagenix). Results are given in IU FVIII/mL, derived from a reference curve generated with an in-house FVIII reference, calibrated against the World Health Organization standard.

FVIII antigen assay

Human FVIII antigen levels in mouse plasma were analyzed by commercial ELISA (Asserachrom VIII:Ag Kit; Diagnostica Stago) per the manufacturer's manual.

Tail tip bleeding assay

The efficacy of TAK-754 was determined by measuring the total blood loss in mice,^{[66](#)} whereby animals were anesthetized (100 mg/kg ketamine and 10 mg/kg xylazine, intraperitoneally) and 2 mm of the tail tip was cut off. Blood was collected over an observation period of 60 min; blood loss was measured gravimetrically.

In vitro biopotency assay

TAK-754 biopotency was assessed *in vitro* using the human hepatic cell line HepG2.^{[46](#)} After treatment of cells with 2 mM hydroxyurea for 22 h, the cells were infected with AAV8-FVIII vectors in F17 medium (Thermo Fisher Scientific) containing 10 µg/mL von Willebrand factor (Baxalta) and 5 µM 5-(*N*-ethyl-*N*-isopropyl)-Amiloride (Sigma). During incubation (96 h), FVIII was expressed and released into the cell supernatant. FVIII activity was determined by chromogenic endpoint measurement, as described for the *in vivo* FVIII biopotency assay. A reference curve of AAV8-FVIII vector material was based on AAV8-ELISA titer.

Neutralizing BDD-FVIII antibody assay

The analysis was based on the Nijmegen modification of the Bethesda assay.⁶⁷ Briefly, the test sample was mixed with a test base (containing BDD-rFVIII), and the loss in FVIII activity upon incubation was measured. The relative loss in activity is correlated to the inhibitor concentration in the sample; results are reported in Bethesda units per milliliter.

Safety evaluation and biodistribution study in hemostatically normal mice

Assessment of toxicity was based on clinical signs, body weight, food consumption, ophthalmology, and clinical and anatomic pathology evaluations. Complete necropsies were performed on five animals from each cohort, with macroscopic abnormalities for all tissues, organ weights, and microscopic examinations recorded. Tissues were collected for biodistribution assessment from a further five animals from each cohort. Blood was collected pre-dose and at necropsy ($n = 5$) for FVIII activity, FVIII Ag, binding anti-BDD-FVIII antibodies, neutralizing anti-BDD-FVIII antibodies, and binding anti-AAV8 antibodies.

Vector IS analysis

We used 25 mg of AAV-treated liver tissues for fully automated DNA isolation using Qiagen spin columns on the QIAcube robotic system. Vector copy numbers were determined by vector-specific qPCR. ISs were analyzed using (nr) and standard LAM-PCR,⁶⁸ which identifies genomic sequences flanking the integrated AAV vector DNA. (nr)LAM-PCR amplicons were sequenced after sample preparation on a MiSeq instrument. Data were processed by (semi-) automated bioinformatics data mining.

Statistical methods

Graphs and statistical analyses were created with GraphPad Prism 6 software. Student's t test, one-way or two-way ANOVA, followed by Holm-Sidak post hoc test was used for the statistical analysis as appropriate. Values are presented as the mean \pm SEM, and $p < 0.05$ was considered to be statistically significant.

Data availability

All data are included in the paper or the [supplemental information](#). Reasonable additional requests may be made of the corresponding author Friedrich Scheiflinger.

Acknowledgments

The study and medical writing support were funded by Baxalta Innovations GmbH, a Takeda company (Vienna, Austria) and Baxalta US Inc., a Takeda company (Lexington, MA, USA). Medical writing support was provided by Isobel Lever, PhD, of Excel Medical Affairs (Fairfield, CT, USA).

Author contributions

J.L. Conceptualization, J.L., F.G.F., W.H., and H.R. Methodology, J.L., J.M., I.G.-F., and M.K. Investigation, J.L., F.H., and I.G.-F. Data curation, M.W. Visualization, J.L., M.W., and F.H. Validation, M.W., J.M., and M.S. Writing – original draft, H.R. Writing – review & editing, F.S. and W.H. Supervision, M.S., F.G.F., M.K., W.H., and H.R. Project administration, F.H. and M.S. Funding acquisition, F.S.

Declaration of interests

M.W. is an employee of Baxalta Innovations GmbH, a member of the Takeda group of companies. J.L., F.H., J.M., M.S., F.G.F., M.K., F.S., W.H., and H.R. were employees of Baxalta Innovations GmbH, a member of the Takeda group of companies, at the time of the study. I.G.-F. was an employee of Genewerk at the time of the study.

Footnotes

Supplemental information can be found online at <https://doi.org/10.1016/j.omtm.2025.101424> .

Supplemental information

Document S1. Figures S1–S4 and Tables S1 and S2

[mmc1.pdf](#) (928.9KB, pdf)

Document S2. Article plus supplemental information

[mmc2.pdf](#) (3.9MB, pdf)

References

1. Mannucci P.M., Tuddenham E.G. The hemophilias - from royal genes to gene therapy. *N. Engl. J. Med.* 2001;344:1773–1779. doi: 10.1056/NEJM200106073442307. [[DOI](#)] [[PubMed](#)] [[Google Scholar](#)]
2. Furie B., Furie B.C. The molecular basis of blood coagulation. *Cell.* 1988;53:505–518. doi: 10.1016/0092-8674(88)90567-3. [[DOI](#)] [[PubMed](#)] [[Google Scholar](#)]
3. Giannelli F., Green P.M. The molecular basis of haemophilia A and B. *Baillieres Clin. Haematol.* 1996;9:211–228. doi: 10.1016/s0950-3536(96)80059-x. [[DOI](#)] [[PubMed](#)] [[Google Scholar](#)]
4. Srivastava A., Santagostino E., Dougall A., Kitchen S., Sutherland M., Pipe S.W., Carcao M., Mahlangu J., Ragni M.V., Windyga J., et al. WFH Guidelines for the Management of Hemophilia, 3rd edition. *Haemophilia.* 2020;26:1–158. doi: 10.1111/hae.14046. [[DOI](#)] [[PubMed](#)] [[Google Scholar](#)]
5. Manco-Johnson M.J., Soucie J.M., Gill J.C., Joint Outcomes Committee of the Universal Data Collection, US Hemophilia Treatment Center Network Prophylaxis usage, bleeding rates, and joint outcomes of hemophilia, 1999 to 2010: a surveillance project. *Blood.* 2017;129:2368–2374. doi: 10.1182/blood-2016-02-683169. [[DOI](#)] [[PMC free article](#)] [[PubMed](#)] [[Google Scholar](#)]
6. Pipe S.W., Shima M., Lehle M., Shapiro A., Chebon S., Fukutake K., Key N.S., Portron A., Schmitt C., Podolak-Dawidziak M., et al. Efficacy, safety, and pharmacokinetics of emicizumab prophylaxis given every 4 weeks in people with haemophilia A (HAVEN 4): a multicentre, open-label, non-randomised phase 3 study. *Lancet. Haematol.* 2019;6:e295–e305. doi: 10.1016/S2352-3026(19)30054-7. [[DOI](#)] [[PubMed](#)] [[Google Scholar](#)]
7. Bueren J.A., Auricchio A. Advances and challenges in the development of gene therapy medicinal products for rare diseases. *Hum. Gene Ther.* 2023;34:763–775. doi: 10.1089/hum.2023.152. [[DOI](#)] [[PubMed](#)] [[Google Scholar](#)]
8. Mannucci P.M. Hemophilia treatment innovation: 50 years of progress and more to come. *J. Thromb. Haemost.* 2023;21:403–412. doi: 10.1016/j.jtha.2022.12.029. [[DOI](#)] [[PubMed](#)] [[Google Scholar](#)]
9. McIntosh J., Lenting P.J., Rosales C., Lee D., Rabbanian S., Raj D., Patel N., Tuddenham E.G.D., Christophe O.D., McVey J.H., et al. Therapeutic levels of FVIII following a single peripheral vein administration of rAAV vector encoding a novel human factor VIII variant. *Blood.* 2013;121:3335–3344. doi: 10.1182/blood-2012-10-462200. [[DOI](#)] [[PMC free article](#)] [[PubMed](#)] [[Google Scholar](#)]
10. Bunting S., Zhang L., Xie L., Bullens S., Mahimkar R., Fong S., Sandza K., Harmon D., Yates B., Handyside B., et al. Gene therapy with BMN 270 results in therapeutic levels of FVIII in mice and primates

and normalization of bleeding in hemophilic mice. *Mol. Ther.* 2018;26:496–509. doi: 10.1016/j.ymthe.2017.12.009. [[DOI](#)] [[PMC free article](#)] [[PubMed](#)] [[Google Scholar](#)]

11. Brown H.C., Zakas P.M., George S.N., Parker E.T., Spencer H.T., Doering C.B. Target-cell-directed bioengineering approaches for gene therapy of Hemophilia A. *Mol. Ther. Methods Clin. Dev.* 2018;9:57–69. doi: 10.1016/j.omtm.2018.01.004. [[DOI](#)] [[PMC free article](#)] [[PubMed](#)] [[Google Scholar](#)]

12. Jiang H., Lillicrap D., Patarroyo-White S., Liu T., Qian X., Scallan C.D., Powell S., Keller T., McMurray M., Labelle A., et al. Multiyear therapeutic benefit of AAV serotypes 2, 6, and 8 delivering factor VIII to hemophilia A mice and dogs. *Blood.* 2006;108:107–115. doi: 10.1182/blood-2005-12-5115. [[DOI](#)] [[PubMed](#)] [[Google Scholar](#)]

13. Pierce G.F., Fong S., Long B.R., Kaczmarek R. Deciphering conundrums of adeno-associated virus liver-directed gene therapy: focus on hemophilia. *J. Thromb. Haemost.* 2024;22:1263–1289. doi: 10.1016/j.jtha.2023.12.005. [[DOI](#)] [[PubMed](#)] [[Google Scholar](#)]

14. Rangarajan S., Walsh L., Lester W., Perry D., Madan B., Laffan M., Yu H., Vettermann C., Pierce G.F., Wong W.Y., Pasi K.J. AAV5-Factor VIII gene transfer in severe Hemophilia A. *N. Engl. J. Med.* 2017;377:2519–2530. doi: 10.1056/NEJMoa1708483. [[DOI](#)] [[PubMed](#)] [[Google Scholar](#)]

15. Pasi K.J., Rangarajan S., Mitchell N., Lester W., Symington E., Madan B., Laffan M., Russell C.B., Li M., Pierce G.F., Wong W.Y. Multiyear follow-up of AAV5-hFVIII-SQ gene therapy for Hemophilia A. *N. Engl. J. Med.* 2020;382:29–40. doi: 10.1056/NEJMoa1908490. [[DOI](#)] [[PubMed](#)] [[Google Scholar](#)]

16. Fong S., Handyside B., Sihn C.-R., Liu S., Zhang L., Xie L., Murphy R., Galicia N., Yates B., Minto W.C., et al. Induction of ER Stress by an AAV5 BDD FVIII construct is dependent on the strength of the hepatic-specific promoter. *Mol. Ther. Methods Clin. Dev.* 2020;18:620–630. doi: 10.1016/j.omtm.2020.07.005. [[DOI](#)] [[PMC free article](#)] [[PubMed](#)] [[Google Scholar](#)]

17. Ozelo M.C., Mahlangu J., Pasi K.J., Giermasz A., Leavitt A.D., Laffan M., Symington E., Quon D.V., Wang J.-D., Peerlinck K., et al. Valoctocogene Roxaparvovec gene therapy for Hemophilia A. *N. Engl. J. Med.* 2022;386:1013–1025. doi: 10.1056/NEJMoa2113708. [[DOI](#)] [[PubMed](#)] [[Google Scholar](#)]

18. Konkle B.A., Walsh C.E., Escobar M.A., Josephson N.C., Young G., von Drygalski A., McPhee S.W.J., Samulski R.J., Bilic I., de la Rosa M., et al. BAX 335 hemophilia B gene therapy clinical trial results: potential impact of CpG sequences on gene expression. *Blood.* 2021;137:763–774. doi: 10.1182/blood.2019004625. [[DOI](#)] [[PMC free article](#)] [[PubMed](#)] [[Google Scholar](#)]

19. Manno C.S., Pierce G.F., Arruda V.R., Glader B., Ragni M., Rasko J.J., Ozelo M.C., Hoots K., Blatt P., Konkle B., et al. Successful transduction of liver in hemophilia by AAV-Factor IX and limitations imposed by the host immune response. *Nat. Med.* 2006;12:342–347. doi: 10.1038/nm1358. [[DOI](#)] [[PubMed](#)] [[Google](#)]

20. Ertl H.C.J. Immunogenicity and toxicity of AAV gene therapy. *Front. Immunol.* 2022;13 doi: 10.3389/fimmu.2022.975803. [[DOI](#)] [[PMC free article](#)] [[PubMed](#)] [[Google Scholar](#)]
21. Mingozzi F., High K.A. Immune responses to AAV in clinical trials. *Curr. Gene Ther.* 2011;11:321–330. doi: 10.2174/156652311796150354. [[DOI](#)] [[PubMed](#)] [[Google Scholar](#)]
22. Wright J.F. Codon modification and PAMPs in clinical AAV Vectors: The tortoise or the hare? *Mol. Ther.* 2020;28:701–703. doi: 10.1016/j.ymthe.2020.01.026. [[DOI](#)] [[PMC free article](#)] [[PubMed](#)] [[Google Scholar](#)]
23. Kaufman R.J., Pipe S.W., Tagliavacca L., Swaroop M., Moussalli M. Biosynthesis, assembly and secretion of coagulation factor VIII. *Blood Coagul. Fibrinolysis.* 1997;8:S3–S14. [[PubMed](#)] [[Google Scholar](#)]
24. Faust S.M., Bell P., Cutler B.J., Ashley S.N., Zhu Y., Rabinowitz J.E., Wilson J.M. CpG-depleted adeno-associated virus vectors evade immune detection. *J. Clin. Invest.* 2013;123:2994–3001. doi: 10.1172/JCI68205. [[DOI](#)] [[PMC free article](#)] [[PubMed](#)] [[Google Scholar](#)]
25. Falkner F.G., Horling F., Lengler J., Rottensteiner H., Scheiflinger F. Viral vectors encoding recombinant FVIII expression for gene therapy of hemophilia A. 2019. <https://patentimages.storage.googleapis.com/42/62/15/189de0b30d8e0c/US20190194295A1.pdf> US Patent Application Publication.
26. Colomb-Delsuc M., Raim R., Fiedler C., Reuberger S., Lengler J., Nordström R., Ryner M., Folea I.M., Kraus B., Hernandez Bort J.A., Sintorn I.M. Assessment of the percentage of full recombinant adeno-associated virus particles in a gene therapy drug using CryoTEM. *PLoS One.* 2022;17 doi: 10.1371/journal.pone.0269139. [[DOI](#)] [[PMC free article](#)] [[PubMed](#)] [[Google Scholar](#)]
27. Qian J., Borovok M., Bi L., Kazazian H.H., Jr., Hoyer L.W. Inhibitor antibody development and T cell response to human factor VIII in murine hemophilia A. *Thromb. Haemost.* 1999;81:240–244. [[PubMed](#)] [[Google Scholar](#)]
28. van Helden P.M., Unterthurner S., Hermann C., Schuster M., Ahmad R.U., Schiviz A.N., Weiller M., Antoine G., Turecek P.L., Muchitsch E.M., et al. Maintenance and break of immune tolerance against human factor VIII in a new transgenic hemophilic mouse model. *Blood.* 2011;118:3698–3707. doi: 10.1182/blood-2010-11-316521. [[DOI](#)] [[PubMed](#)] [[Google Scholar](#)]
29. Lundgren T.S., Denning G., Stowell S.R., Spencer H.T., Doering C.B. Pharmacokinetic analysis identifies a factor VIII immunogenicity threshold after AAV gene therapy in hemophilia A mice. *Blood Adv.* 2022;6:2628–2645. doi: 10.1182/bloodadvances.2021006359. [[DOI](#)] [[PMC free article](#)] [[PubMed](#)] [[Google](#)

30. Nault J.-C., Datta S., Imbeaud S., Franconi A., Mallet M., Couchy G., Letouzé E., Pilati C., Verret B., Blanc J.-F., et al. Recurrent AAV2-related insertional mutagenesis in human hepatocellular carcinomas. *Nat. Genet.* 2015;47:1187–1193. doi: 10.1038/ng.3389. [[DOI](#)] [[PubMed](#)] [[Google Scholar](#)]
31. Sandberg H., Almstedt A., Brandt J., Gray E., Holmquist L., Oswaldsson U., Sebring S., Mikaelsson M. Structural and functional characteristics of the B-domain-deleted recombinant factor VIII protein, r-VIII SQ. *Thromb. Haemost.* 2001;85:93–100. [[PubMed](#)] [[Google Scholar](#)]
32. Thomas C.E., Storm T.A., Huang Z., Kay M.A. Rapid uncoating of vector genomes is the key to efficient liver transduction with pseudotyped adeno-associated virus vectors. *J. Virol.* 2004;78:3110–3122. doi: 10.1128/JVI.78.6.3110-3122.2004. [[DOI](#)] [[PMC free article](#)] [[PubMed](#)] [[Google Scholar](#)]
33. Pipe S., Leebeek F.W.G., Ferreira V., Sawyer E.K., Pasi J. Clinical Considerations for Capsid Choice in the Development of Liver-Targeted AAV-Based Gene Transfer. *Mol. Ther. Methods Clin. Dev.* 2019;15:170–178. doi: 10.1016/j.omtm.2019.08.015. [[DOI](#)] [[PMC free article](#)] [[PubMed](#)] [[Google Scholar](#)]
34. Nathwani A.C., Gray J.T., Ng C.Y.C., Zhou J., Spence Y., Waddington S.N., Tuddenham E.G.D., Kemball-Cook G., McIntosh J., Boon-Spijker M., et al. Self-complementary adeno-associated virus vectors containing a novel liver-specific human factor IX expression cassette enable highly efficient transduction of murine and nonhuman primate liver. *Blood.* 2006;107:2653–2661. doi: 10.1182/blood-2005-10-4035. [[DOI](#)] [[PMC free article](#)] [[PubMed](#)] [[Google Scholar](#)]
35. Lisowski L., Dane A.P., Chu K., Zhang Y., Cunningham S.C., Wilson E.M., Nygaard S., Grompe M., Alexander I.E., Kay M.A. Selection and evaluation of clinically relevant AAV variants in a xenograft liver model. *Nature.* 2014;506:382–386. doi: 10.1038/nature12875. [[DOI](#)] [[PMC free article](#)] [[PubMed](#)] [[Google Scholar](#)]
36. Krooss S.A., Dai Z., Schmidt F., Rovai A., Fakhiri J., Dhingra A., Yuan Q., Yang T., Balakrishnan A., Steinbrück L., et al. Ex vivo/In vivo gene editing in hepatocytes using “All-in-One” CRISPR-Adeno-associated virus vectors with a self-linearizing repair template. *iScience.* 2020;23 doi: 10.1016/j.isci.2019.100764. [[DOI](#)] [[PMC free article](#)] [[PubMed](#)] [[Google Scholar](#)]
37. Wu Z., Yang H., Colosi P. Effect of genome size on AAV vector packaging. *Mol. Ther.* 2010;18:80–86. doi: 10.1038/mt.2009.255. [[DOI](#)] [[PMC free article](#)] [[PubMed](#)] [[Google Scholar](#)]
38. Nambiar B., Cornell Sookdeo C., Berthelette P., Jackson R., Piraino S., Burnham B., Nass S., Souza D., O’Riordan C.R., Vincent K.A., et al. Characteristics of minimally oversized Adeno-associated virus vectors encoding human Factor VIII generated using producer cell lines and triple transfection. *Hum. Gene Ther. Methods.* 2017;28:23–38. doi: 10.1089/hgtb.2016.124. [[DOI](#)] [[PMC free article](#)] [[PubMed](#)] [[Google](#)]

39. Monahan P.E., Sun J., Gui T., Hu G., Hannah W.B., Wichlan D.G., Wu Z., Grieger J.C., Li C., Suwanmanee T., et al. Employing a gain-of-function factor IX variant R338L to advance the efficacy and safety of hemophilia B human gene therapy: preclinical evaluation supporting an ongoing adeno-associated virus clinical trial. *Hum. Gene Ther.* 2015;26:69–81. doi: 10.1089/hum.2014.106. [[DOI](#)] [[PMC free article](#)] [[PubMed](#)] [[Google Scholar](#)]
40. Greig J.A., Wang Q., Reicherter A.L., Chen S.-J., Hanlon A.L., Tipper C.H., Clark K.R., Wadsworth S., Wang L., Wilson J.M. Characterization of Adeno-associated viral vector-mediated human Factor VIII gene therapy in Hemophilia A mice. *Hum. Gene Ther.* 2017;28:392–402. doi: 10.1089/hum.2016.128. [[DOI](#)] [[PubMed](#)] [[Google Scholar](#)]
41. Elkouby L., Armour S.M., Toso R., DiPietro M., Davidson R.J., Nguyen G.N., Willet M., Kutza S., Silverberg J., Frick J., et al. Preclinical assessment of an optimized AAV-FVIII vector in mice and non-human primates for the treatment of hemophilia A. *Mol. Ther. Methods Clin. Dev.* 2022;24:20–29. doi: 10.1016/j.omtm.2021.11.005. [[DOI](#)] [[PMC free article](#)] [[PubMed](#)] [[Google Scholar](#)]
42. Kudla G., Lipinski L., Caffin F., Helwak A., Zylicz M. High guanine and cytosine content increases mRNA levels in mammalian cells. *PLoS Biol.* 2006;4:e180. doi: 10.1371/journal.pbio.0040180. [[DOI](#)] [[PMC free article](#)] [[PubMed](#)] [[Google Scholar](#)]
43. Barber G.N. Cytoplasmic DNA innate immune pathways. *Immunol. Rev.* 2011;243:99–108. doi: 10.1111/j.1600-065X.2011.01051.x. [[DOI](#)] [[PubMed](#)] [[Google Scholar](#)]
44. Iwasaki A., Medzhitov R. Control of adaptive immunity by the innate immune system. *Nat. Immunol.* 2015;16:343–353. doi: 10.1038/ni.3123. [[DOI](#)] [[PMC free article](#)] [[PubMed](#)] [[Google Scholar](#)]
45. Gardiner-Garden M., Frommer M. CpG islands in vertebrate genomes. *J. Mol. Biol.* 1987;196:261–282. doi: 10.1016/0022-2836(87)90689-9. [[DOI](#)] [[PubMed](#)] [[Google Scholar](#)]
46. Lengler J., Coulibaly S., Gruber B., Ilk R., Mayrhofer J., Scheifflinger F., Hoellriegl W., Falkner F.G., Rottensteiner H. Development of an in vitro biopotency assay for an AAV8 Hemophilia B gene therapy vector suitable for clinical product release. *Mol. Ther. Methods Clin. Dev.* 2020;17:581–588. doi: 10.1016/j.omtm.2020.03.013. [[DOI](#)] [[PMC free article](#)] [[PubMed](#)] [[Google Scholar](#)]
47. Fong S., Yates B., Sihn C.-R., Mattis A.N., Mitchell N., Liu S., Russell C.B., Kim B., Lawal A., Rangarajan S., et al. Interindividual variability in transgene mRNA and protein production following adeno-associated virus gene therapy for hemophilia A. *Nat. Med.* 2022;28:789–797. doi: 10.1038/s41591-022-01751-0. [[DOI](#)] [[PMC free article](#)] [[PubMed](#)] [[Google Scholar](#)]

48. Yates brid, Keenan W., Razon L., Scheeler S., Liu S., Bunting S., Fong S. Investigating mechanisms of variability of AAV5- hFVIII-SQ expression in vitro. Hum. Gene Ther. 2022;33 A158, P501. [[Google Scholar](#)]
49. Gavin D.K. Advanced topics: successful development of quality cell and gene therapy products. Food and Drug Administration, Center for Biologics Evaluation and Research Web Seminar Series. 2015. <https://www.fda.gov/media/80404/download>
50. Kapelanski-Lamoureux A., Chen Z., Gao Z.-H., Deng R., Lazaris A., Lebeauupin C., Giles L., Malhotra J., Yong J., Zou C., et al. Ectopic clotting factor VIII expression and misfolding in hepatocytes as a cause for hepatocellular carcinoma. Mol. Ther. 2022;30:3542–3551. doi: 10.1016/j.ymthe.2022.10.004. [[DOI](#)] [[PMC free article](#)] [[PubMed](#)] [[Google Scholar](#)]
51. Wang J.-H., Gessler D.J., Zhan W., Gallagher T.L., Gao G. Adeno-associated virus as a delivery vector for gene therapy of human diseases. Signal Transduct. Target. Ther. 2024;9:78. doi: 10.1038/s41392-024-01780-w. [[DOI](#)] [[PMC free article](#)] [[PubMed](#)] [[Google Scholar](#)]
52. Chapin J., Allen G., Álvarez-Román M.T., Ayash-Rashokovsky, López Jaime F.J., Maggiore C., Mingot-Castellano M.E., Raja el K., Rauch A., Susen S. Hemophilia; 2021. Results from a phase 1/2 safety and dose escalation study of TAK-754, an AAV8 vector with a codon optimized B-domain-deleted factor VIII transgene in severe hemophilia A. Issue S2. [[Google Scholar](#)]
53. Chapin J., Ayash-Rashovsky M., Kenniston J., Wagoner M., Wang Q. Research and Practice in Thrombosis and Haemostasis; 2022. A translational analysis of immune components in peripheral blood from severe hemophilia A patients treated with TAK-754, an AAV8 vector with a codon-optimized B-domain-deleted factor VIII transgene. Issue S1. [[Google Scholar](#)]
54. Wang L., Calcedo R., Bell P., Lin J., Grant R.L., Siegel D.L., Wilson J.M. Impact of pre-existing immunity on gene transfer to nonhuman primate liver with adeno-associated virus 8 vectors. Hum. Gene Ther. 2011;22:1389–1401. doi: 10.1089/hum.2011.031. [[DOI](#)] [[PMC free article](#)] [[PubMed](#)] [[Google Scholar](#)]
55. Hurlbut G.D., Ziegler R.J., Nietupski J.B., Foley J.W., Woodworth L.A., Meyers E., Bercury S.D., Pande N.N., Souza D.W., Bree M.P., et al. Preexisting immunity and low expression in primates highlight translational challenges for liver-directed AAV8-mediated gene therapy. Mol. Ther. 2010;18:1983–1994. doi: 10.1038/mt.2010.175. [[DOI](#)] [[PMC free article](#)] [[PubMed](#)] [[Google Scholar](#)]
56. Colella P., Ronzitti G., Mingozi F. Emerging issues in AAV-mediated in vivo gene therapy. Mol. Ther. Methods Clin. Dev. 2018;8:87–104. doi: 10.1016/j.omtm.2017.11.007. [[DOI](#)] [[PMC free article](#)] [[PubMed](#)] [[Google Scholar](#)]
57. Samelson-Jones B.J., Small J.C., George L.A. Roctavian gene therapy for hemophilia A. Blood Adv.

2024;8:5179–5189. doi: 10.1182/bloodadvances.2023011847. [[DOI](#)] [[PMC free article](#)] [[PubMed](#)] [[Google Scholar](#)]

58. Cao W., Dong B., Horling F., Firman J.A., Lengler J., Klugmann M., de la Rosa M., Wu W., Wang Q., Wei H., et al. Minimal essential human Factor VIII alterations enhance secretion and gene therapy efficiency. *Mol. Ther. Methods Clin. Dev.* 2020;19:486–495. doi: 10.1016/j.omtm.2020.10.013. [[DOI](#)] [[PMC free article](#)] [[PubMed](#)] [[Google Scholar](#)]

59. Brown H.C., Gangadharan B., Doering C.B. Enhanced biosynthesis of coagulation factor VIII through diminished engagement of the unfolded protein response. *J. Biol. Chem.* 2011;286:24451–24457. doi: 10.1074/jbc.M111.238758. [[DOI](#)] [[PMC free article](#)] [[PubMed](#)] [[Google Scholar](#)]

60. Yan C., Costa R.H., Darnell J.E., Jr., Chen J.D., Van Dyke T.A. Distinct positive and negative elements control the limited hepatocyte and choroid plexus expression of transthyretin in transgenic mice. *EMBO J.* 1990;9:869–878. doi: 10.1002/j.1460-2075.1990.tb08184.x. [[DOI](#)] [[PMC free article](#)] [[PubMed](#)] [[Google Scholar](#)]

61. Levitt N., Briggs D., Gil A., Proudfoot N.J. Definition of an efficient synthetic poly(A) site. *Genes Dev.* 1989;3:1019–1025. doi: 10.1101/gad.3.7.1019. [[DOI](#)] [[PubMed](#)] [[Google Scholar](#)]

62. Grieger J.C., Soltys S.M., Samulski R.J. Production of recombinant Adeno-associated virus vectors using suspension HEK293 cells and continuous harvest of vector from the culture media for GMP FIX and FLT1 clinical vector. *Mol. Ther.* 2016;24:287–297. doi: 10.1038/mt.2015.187. [[DOI](#)] [[PMC free article](#)] [[PubMed](#)] [[Google Scholar](#)]

63. Aurnhammer C., Haase M., Muether N., Hausl M., Rauschhuber C., Huber I., Nitschko H., Busch U., Sing A., Ehrhardt A., Baiker A. Universal real-time PCR for the detection and quantification of adeno-associated virus serotype 2-derived inverted terminal repeat sequences. *Hum. Gene Ther. Methods.* 2012;23:18–28. doi: 10.1089/hgtb.2011.034. [[DOI](#)] [[PubMed](#)] [[Google Scholar](#)]

64. Fagone P., Wright J.F., Nathwani A.C., Nienhuis A.W., Davidoff A.M., Gray J.T. Systemic errors in quantitative polymerase chain reaction titration of self-complementary adeno-associated viral vectors and improved alternative methods. *Hum. Gene Ther. Methods.* 2012;23:1–7. doi: 10.1089/hgtb.2011.104. [[DOI](#)] [[PMC free article](#)] [[PubMed](#)] [[Google Scholar](#)]

65. Bi L., Lawler A.M., Antonarakis S.E., High K.A., Gearhart J.D., Kazazian H.H., Jr. Targeted disruption of the mouse factor VIII gene produces a model of haemophilia A. *Nat. Genet.* 1995;10:119–121. doi: 10.1038/ng0595-119. [[DOI](#)] [[PubMed](#)] [[Google Scholar](#)]

66. Greene T.K., Schiviz A., Hoellriegel W., Poncz M., Muchitsch E.-M., Animal Models Subcommittee of the Scientific And Standardization Committee Of The Isth Towards a standardization of the murine tail bleeding

model. J. Thromb. Haemost. 2010;8:2820–2822. doi: 10.1111/j.1538-7836.2010.04084.x. [[DOI](#)] [[PubMed](#)] [[Google Scholar](#)]

67. Verbruggen B., Novakova I., Wessels H., Boezeman J., van den Berg M., Mauser-Bunschoten E. The Nijmegen modification of the Bethesda assay for factor VIII:C inhibitors: improved specificity and reliability. Thromb. Haemost. 1995;73:247–251. [[PubMed](#)] [[Google Scholar](#)]

68. Wang W., Bartholomae C.C., Gabriel R., Deichmann A., Schmidt M. The LAM-PCR method to sequence LV integration sites. Methods Mol. Biol. 2016;1448:107–120. doi: 10.1007/978-1-4939-3753-0_9. [[DOI](#)] [[PubMed](#)] [[Google Scholar](#)]

Associated Data

This section collects any data citations, data availability statements, or supplementary materials included in this article.

Supplementary Materials

Document S1. Figures S1–S4 and Tables S1 and S2

[mmc1.pdf](#) (928.9KB, pdf)

Document S2. Article plus supplemental information

[mmc2.pdf](#) (3.9MB, pdf)

Data Availability Statement

All data are included in the paper or the [supplemental information](#). Reasonable additional requests may be made of the corresponding author Friedrich Scheifflinger.

Articles from Molecular Therapy. Methods & Clinical Development are provided here courtesy of
American Society of Gene & Cell Therapy